Nanometallurgy in Solution: Organometallic Synthesis of Intermetallic Pd–Ga Colloids and their Activity in Semi-Hydrogenation Catalysis.

Lena Staiger[1], Tim Kratky[2], Sebastian Günther[2], Alexander Urstoeger[3], Michael Schuster[3], Ondrej Tomanek[4], Radek Zboril[4], Richard W. Fischer[5], Roland A. Fischer[1,*] and Mirza Cokoja[1,*]

[1] Chair of Inorganic and Metal-Organic Chemistry, Catalysis Research Center and Department of Chemistry, Technical University of Munich, Ernst-Otto-Fischer-Straße 1, D-85747 Garching bei München, Germany. Tel: +49 89 289 13478; e-mail: mirza.cokoja@tum.de; roland.fischer@tum.de.

[2] Chair of Physical Chemistry with Focus on Catalysis, Catalysis Research Center and Department of Chemistry, Technical University of Munich, Garching bei München, Germany.

[3] Working Group Analytical Chemistry, Technical University of Munich, Garching bei München, Germany.

[4] Regional Center of Advanced Technologies and Materials RCPTM, Olomouc, Czech Republic.

[5] Clariant Produkte (Deutschland) GmbH, Bruckmühl, Germany.

Supporting Information

Content

1. Characterization of $Pd_{1-x}Ga_x$ (x = 0.67, 0.5, 0.33) colloids

NMR spectroscopy

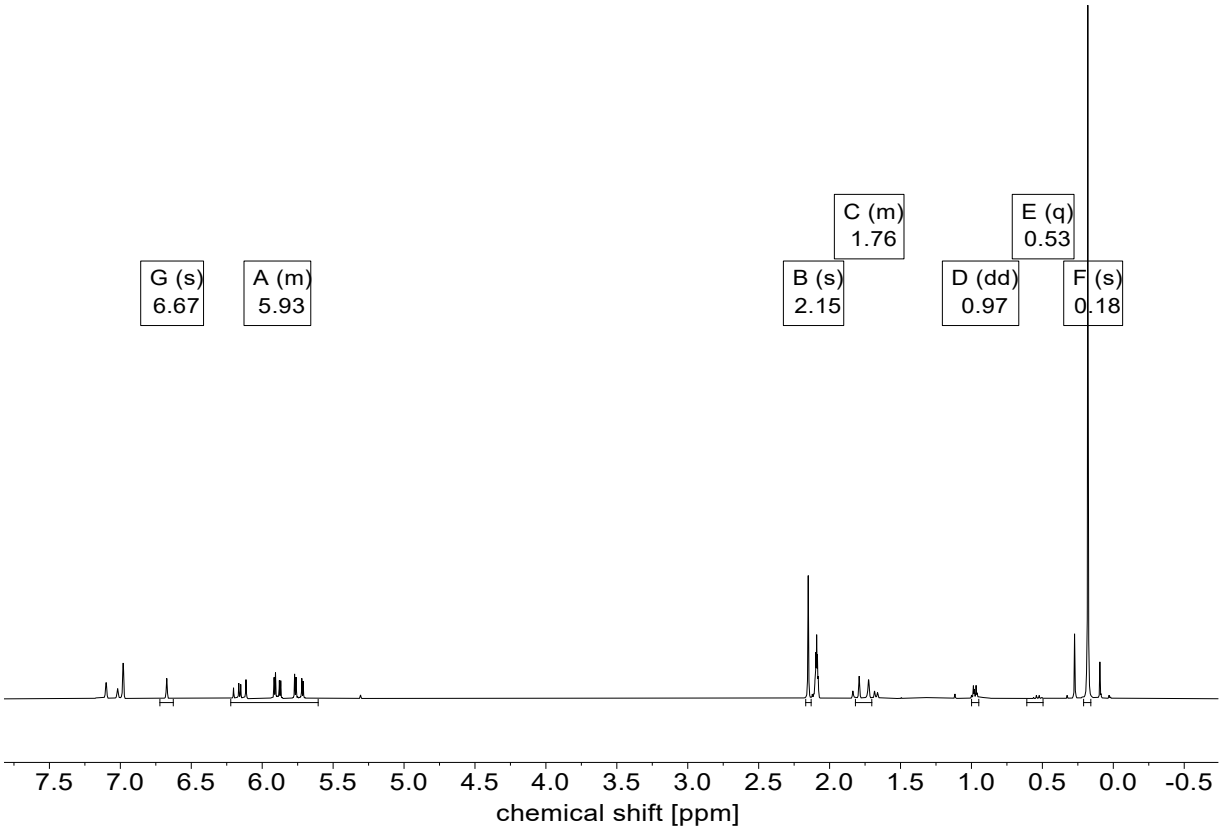

Figure S1. Representative ^{1}H NMR spectra (toluene-d_8) of colloidal $Pd_{1-x}Ga_x$ NPs. ^{1}H NMR (400 MHz, toluene-d_8): 6.67 (s, 3H, mesitylene as internal standard, CH), 5.93 (m, 6H, dvds, CH, CH_2), 2.15 (s, 9H, mesitylene as internal standard, CH_3), 1.76 (m, Cp*H, 12H, CH_3), 0.97 (d, Cp*H, 3H, CH_3), 0.53 (q, Cp*H, 1H, CH), 0.18 (s, dvds, 12H, CH_3). Signals of unreacted GaCp* were not detected for all samples.

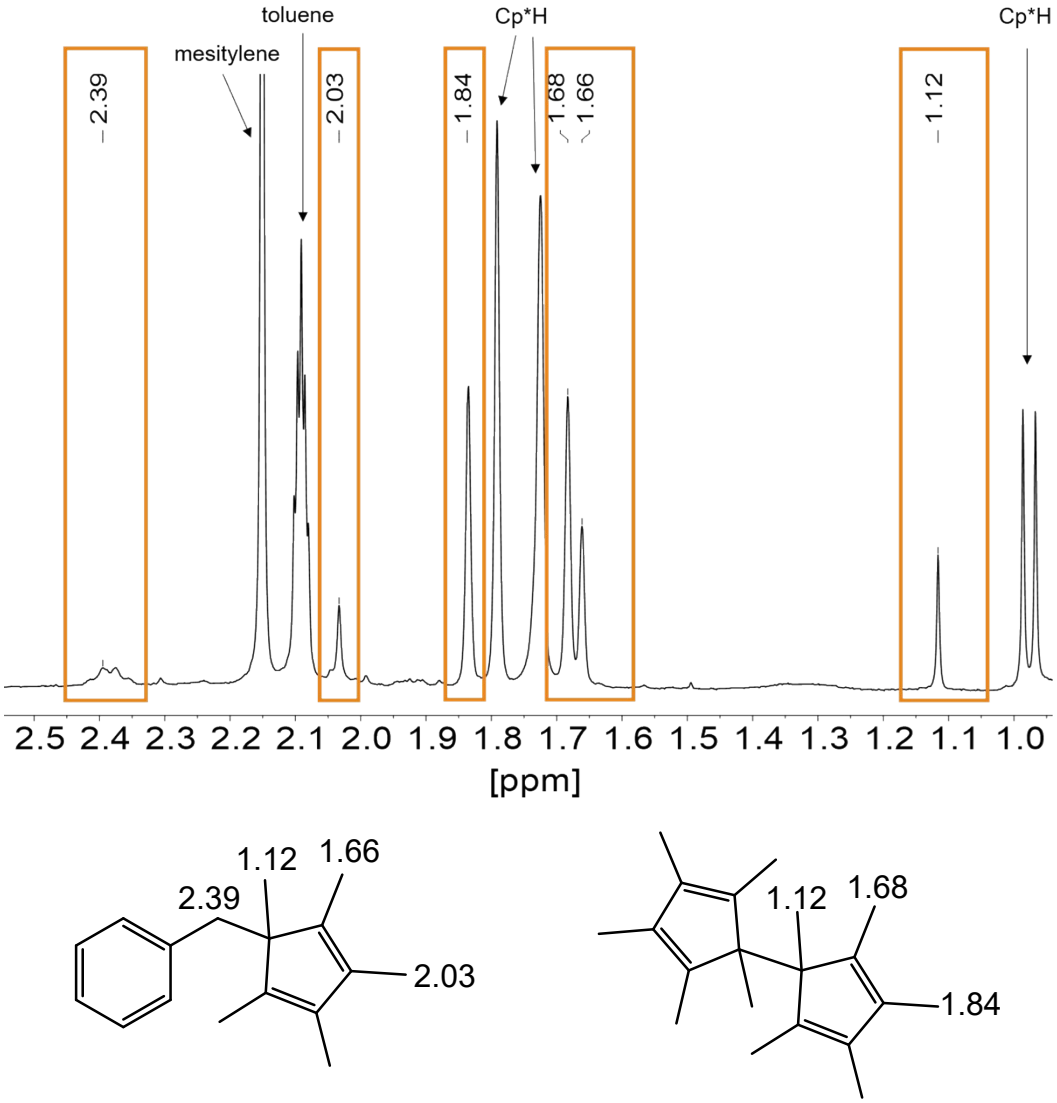

Figure S2. Zoom-in of a representative ^{1}H NMR spectra (toluene-d_8) of colloidal $Pd_{1-x}Ga_x$ NPs showing the signals of C-C coupling products (orange marked). Note that due to overlapping signals and weak signal intensities, a distinct signal assignment is not possible.

GC-MS measurements

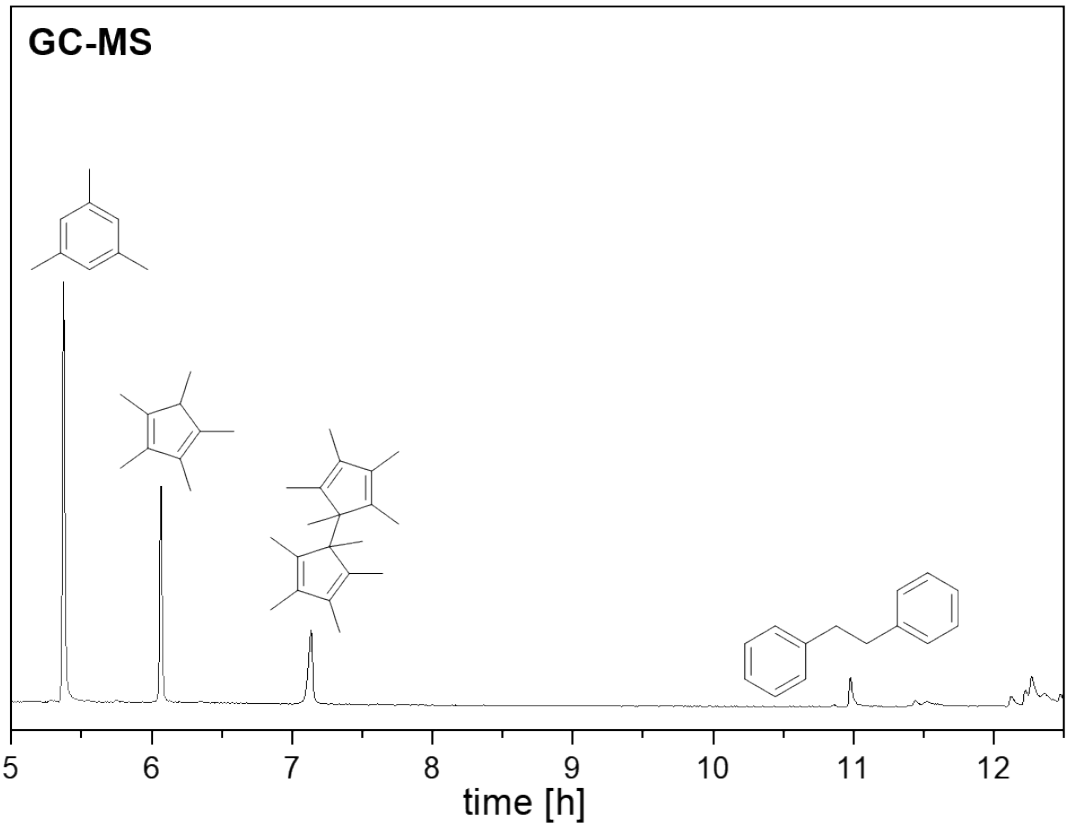

Figure S3. Representative GC chromatogram of colloidal $Pd_{1-x}Ga_x$ NPs showing mesitylene as internal standard and products of a C-H activation reactivity.

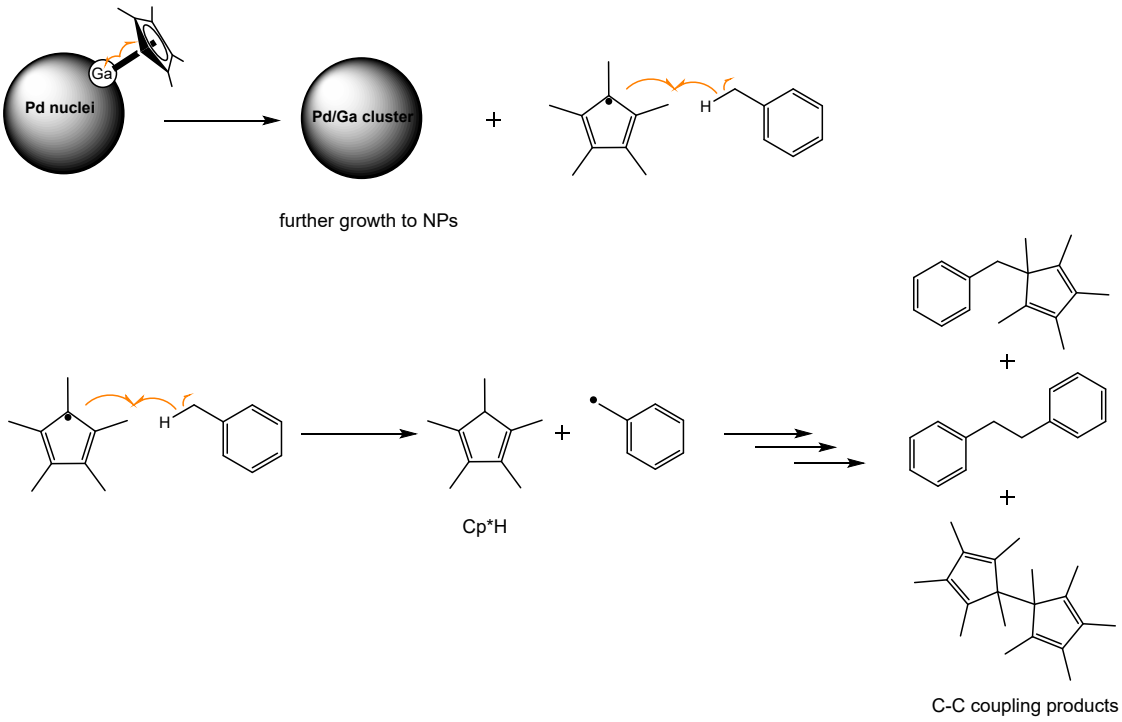

Figure S4. Proposed reaction mechanism of $Pd_{1-x}Ga_x$ NP formation by a radical C-C coupling mechanism.

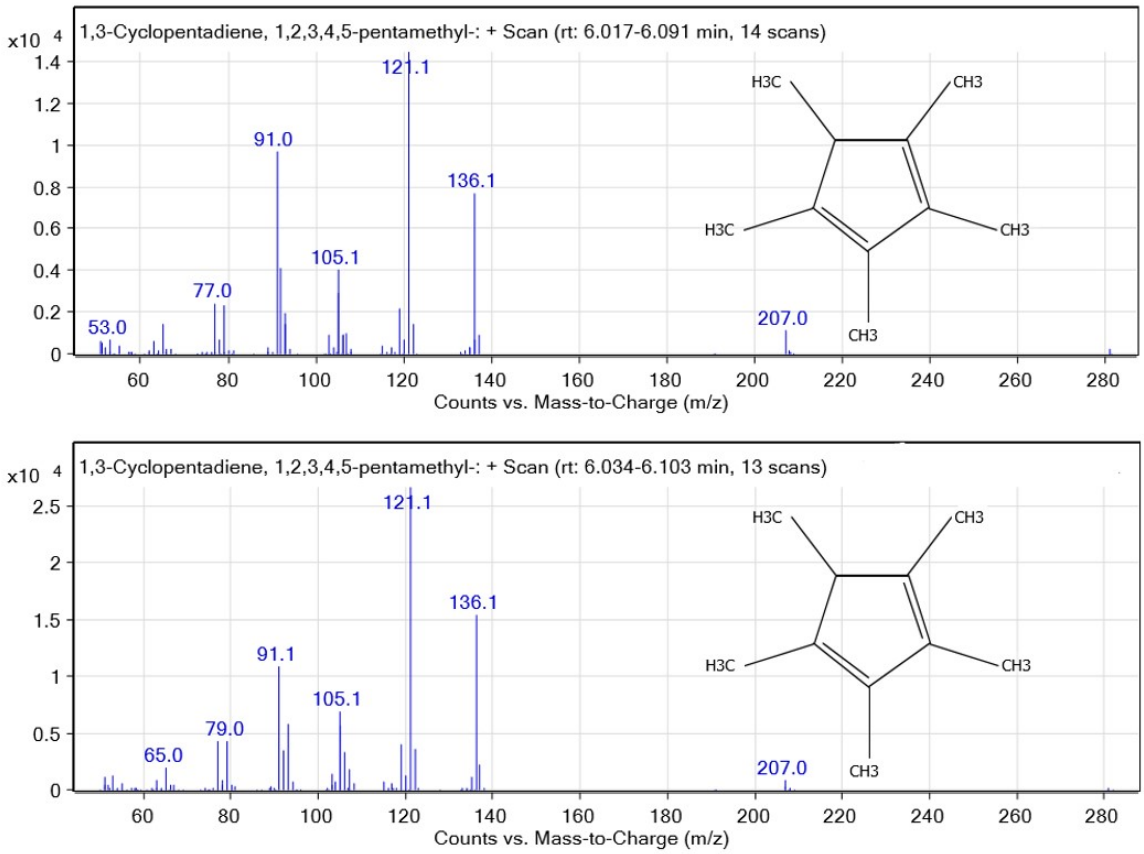

Figure S5. GC-MS mass spectra of Cp*H after the targeted decomposition experiments of $Pd_{0.5}Ga_{0.5}$ colloids with H_2O (above) and D_2O (bottom) showing no differences.

LIFDI-MS measurements

Table S1. Measured and calculated signals of LIFDI-MS measurements during the synthesis of $Pd_{0.5}Ga_{0.5}$ and $Pd_{0.33}Ga_{0.67}$ colloids. Most intense signals are marked in bold.

Applied Pd/Ga ratio	Chemical formula	Calculated m/z [a.u.]	Measured m/z [a.u.]	Temperature [°C]
1:1	$[Pd_2Ga(dvds)(toluene)_2]$	649.3	649.2	-20
1:1	$[Pd_3Ga_3]Cp^*$	663.6	665.1	-20
1:1	**$[Pd_3Ga_4]Cp^*_3dvds$**	1190	1190.1	-10
1:1	$[Pd_4Ga_4]Cp^*_3dvds$	1296	1294.7	-10
1:1	$[Pd_4Ga_5]Cp^*_4tol_2$	1497	1496.6	-10
1:1	**$[Pd_4Ga_5]Cp^*_4dvds$**	1500	1501.2	-10
1:1	**$[Pd_3Ga_3]Cp^*_4(dvds)_3H_4$**	1632	1632.8	-10
1:1	$[Pd_4Ga_3]Cp^*_4(dvds)_3H_4$	1739	1738.8	-10
1:2	$PdGa_4Cp^*_3H_2$	792	792.5	-20
1:2	$PdGa_3Cp^*(dvds)_2H_3$	828	827.5	-20
1:2	$PdGa_4Cp^*(dvds)_2H_4$	897	897.5	-20
1:2	$PdGa_5Cp^*_4H_2$	998	997.9	-20
1:2	$PdGa_3Cp^*(dvds)_3H_2$	1012	1012.1	-20
1:2	$Pd_2Ga_4Cp^*_4H$	1034	1033.9	-20
1:2	$Pd_2Ga_4Cp^*_3(dvds)H_2$	1085	1085.1	-20
1:2	**$Pd_2Ga_5Cp^*_4$**	1102	1102.1	-20
1:2	$Pd_2Ga_4Cp^*_2(dvds)_2H_3$	1138	1138.7	-20
1:2	$Pd_3Ga_3Cp^*_2(dvds)_2$	1170	1170.3	-20
1:2	**$Pd_3Ga_4Cp^*_3(dvds)$**	1190	1190.0	-20
1:2	$Pd_2Ga_5Cp^*_2(dvds)_2H_4$	1209	1208.6	-20
1:2	$Pd_4Ga_5Cp^*_4$	1308	1307.9	-20
1:2	$Pd_2Ga_5Cp^*_3(dvds)_2H_3$	1344	1343.7	-20
1:2	$Pd_5Ga_{10}(dvds)$	1413	1414.1	-20
1:2	**$Pd_4Ga_5Cp^*_4(dvds)$**	1500	1500.7	-20
1:2	$Pd_4Ga_6Cp^*_5$	1520	1519.9	-20
1:2	$Pd_3Ga_3Cp^*_2(dvds)$	985	984.8	-10
1:2	$PdGa_3Cp^*(dvds)_3H_2$	1012	1012.1	-10
1:2	$Pd_3Ga_3Cp^*(dvds)_2H_3$	1038	1037.7	-10
1:2	$Pd_3Ga_3Cp^*_2*(dvds)tol$	1077	1077.9	-10
1:2	$Pd_3Ga_3Cp^*_3dvds$	1118	1118.1	-10
1:2	**$Pd_3Ga_3Cp^*_2dvds_2$**	1171	1171.5	-10

1:2	**$Pd_3Ga_4Cp^*_3dvds$**	1190	1190.3	-10
1:2	**$Pd_3Ga_3Cp^*_3(dvds)_2$**	1307	1306.8	-10
1:2	**$Pd_4Ga_{13}Cp^*$**	1467	1467.7	-10
1:2	**$Pd_4Ga_5Cp^*_4dvds$**	1501	1501.6	-10
1:2	$Ga_4Cp^*_5(dvds)_3H_4$	1513	1513.8	-10
1:2	$PdGa_8Cp^*(dvds)_4H_3$	1546	1545.9	-10
1:2	$Pd_4Ga_7Cp^*_4(dvds)H_3$	1643	1643.3	-10

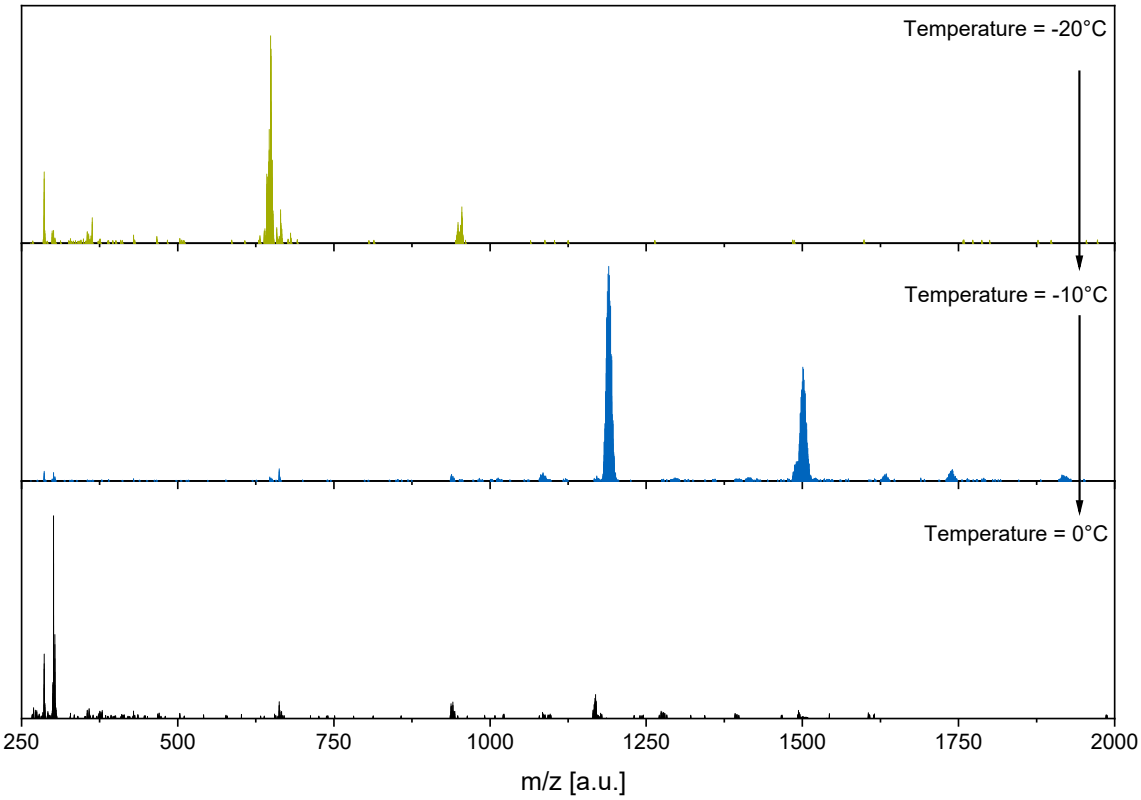

Figure S6. Representative LIFDI-MS spectra monitoring the cluster formation and deformation during synthesis of colloidal $Pd_{0.5}Ga_{0.5}$ NPs at various temperatures (top: -20°C, middle: -10°C, bottom: 0°C) by a slow warming up of the reaction mixture.

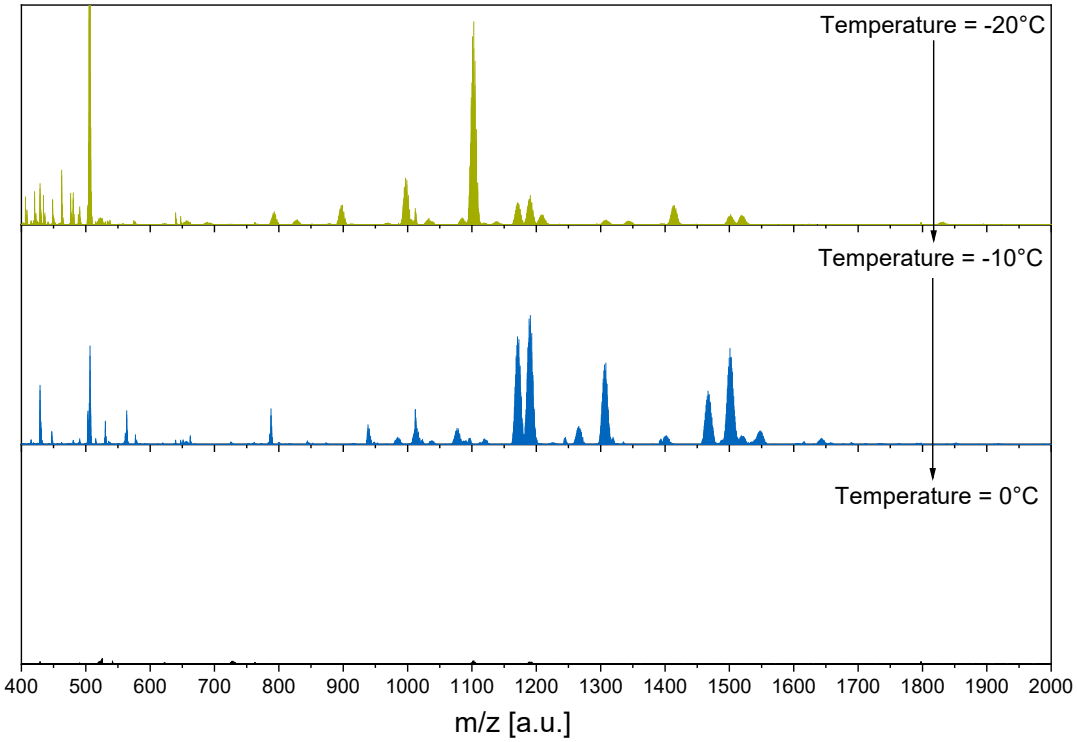

Figure S7. Representative LIFDI-MS spectra monitoring the cluster formation and deformation during synthesis of colloidal $Pd_{0.33}Ga_{0.67}$ NPs at various temperatures (top: -20°C, middle: -10°C, bottom: 0°C) by a slow warming up of the reaction mixture.

HR-TEM measurements

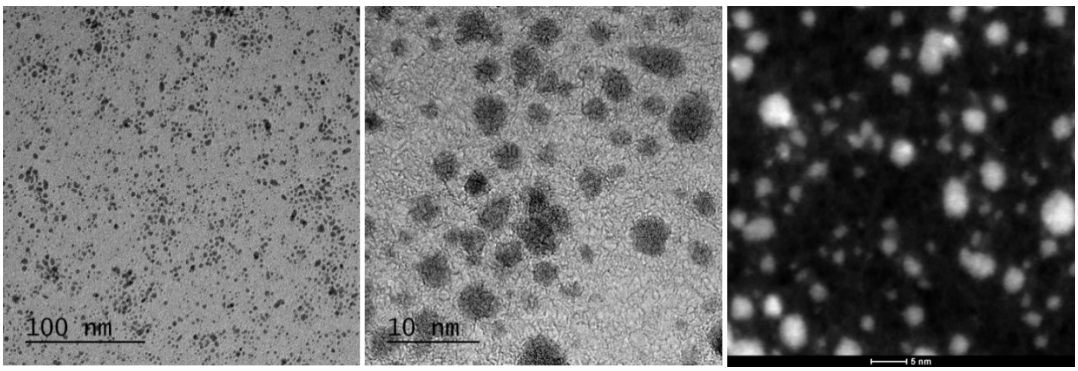

Figure S8. HR-TEM image (overview and increased magnification) and HAADF of $Pd_{0.9}Ga_{0.1}$ colloid.

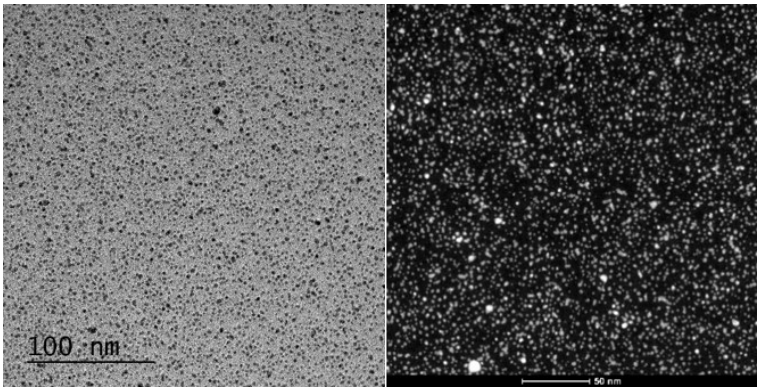

Figure S9. HR-TEM image and HAADF of $Pd_{0.67}Ga_{0.33}$ colloids.

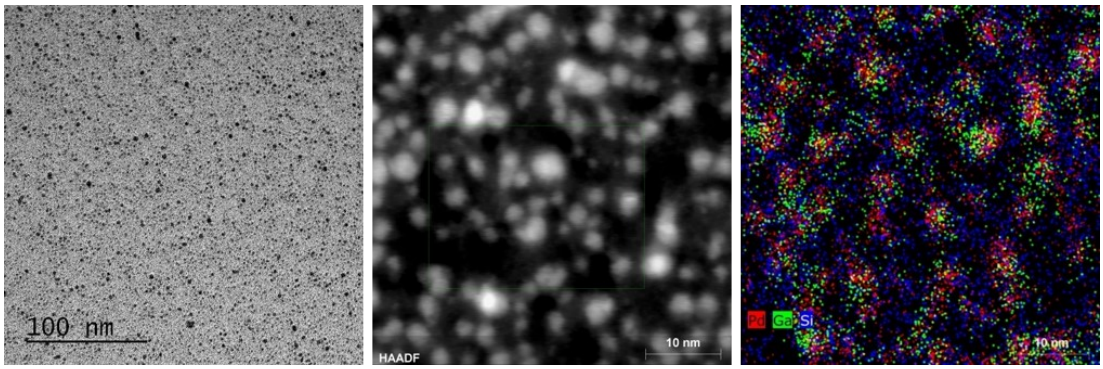

Figure S10. HR-TEM image, HAADF and elemental mapping of $Pd_{0.5}Ga_{0.5}$ colloids showing a homogeneous distribution of Pd and Ga.

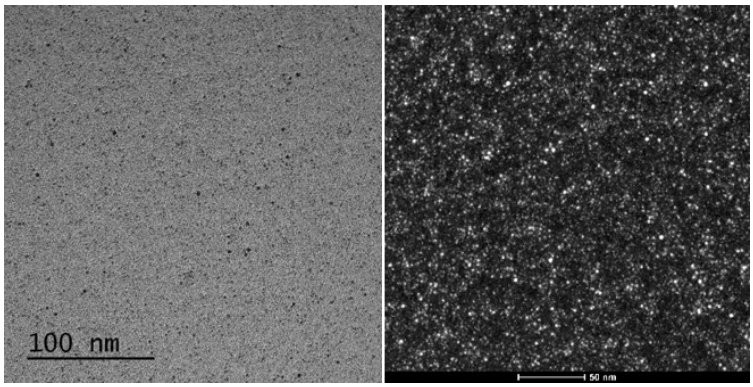

Figure S11. HR-TEM image and HAADF of $Pd_{0.33}Ga_{0.67}$ colloids.

DLS measurements

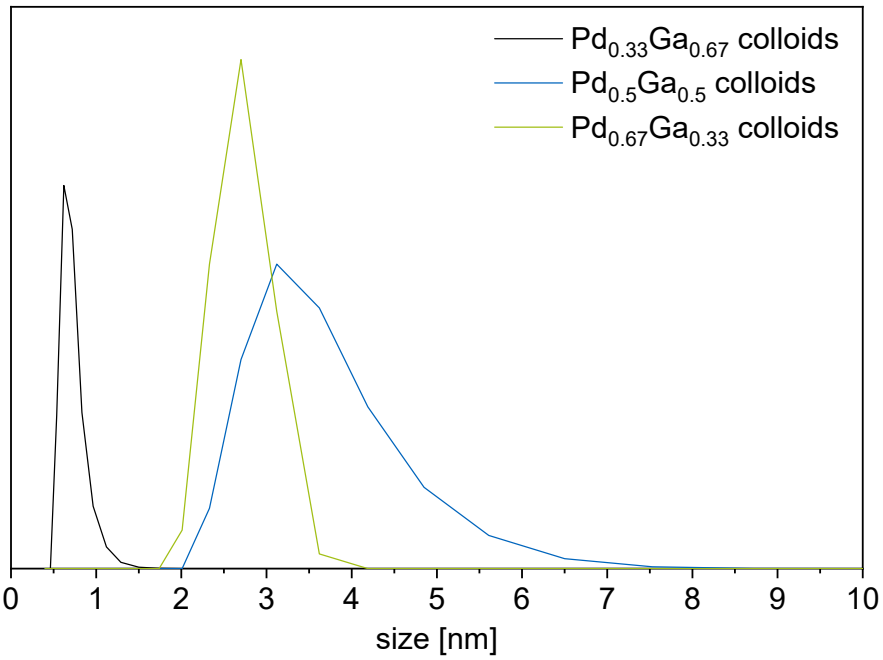

Figure S12. DLS measurements of all $Pd_{1-x}Ga_x$ samples at 0°C.

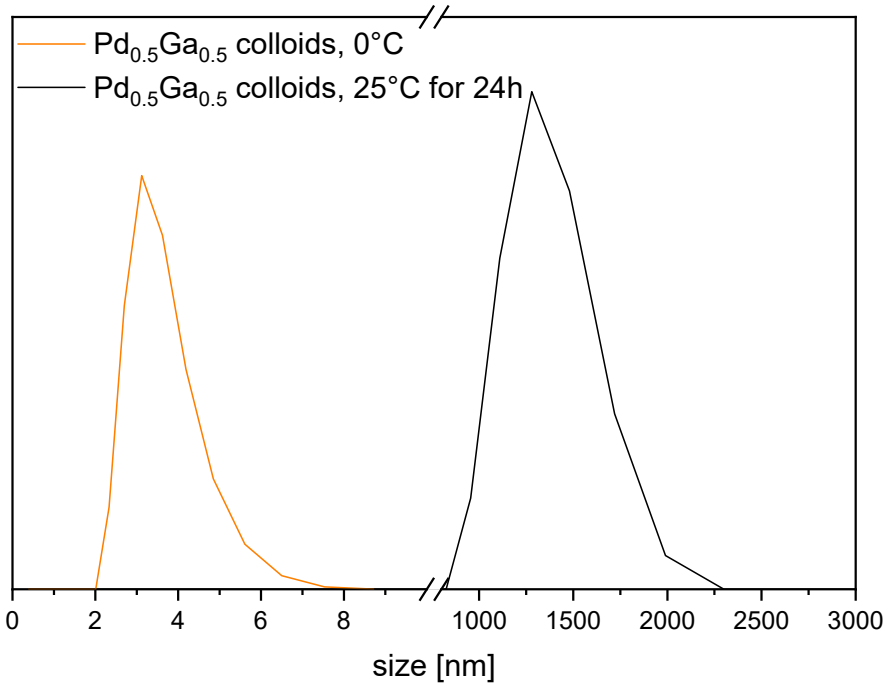

Figure S13. DLS measurements of $Pd_{0.5}Ga_{0.5}$ colloids at 0°C and after 24 h stored at 25°C showing agglomeration with concomitant precipitation.

IR measurements

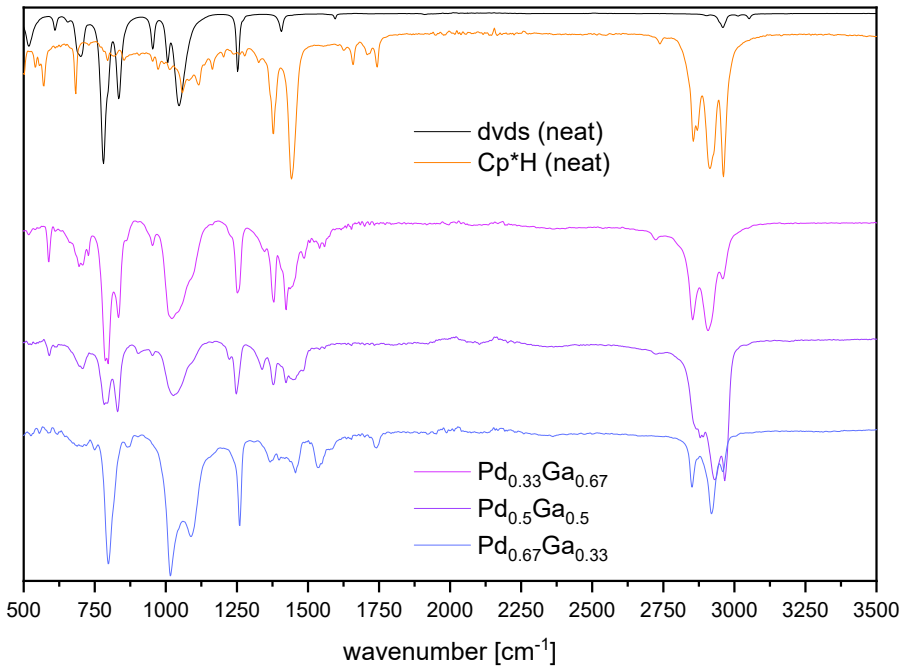

Figure S14. ATR FT-IR measurement of the $Pd_{1-x}Ga_x$ colloids (bottom traces) and pure dvds and Cp*H as reference (upper traces, black and orange).

Raman measurements

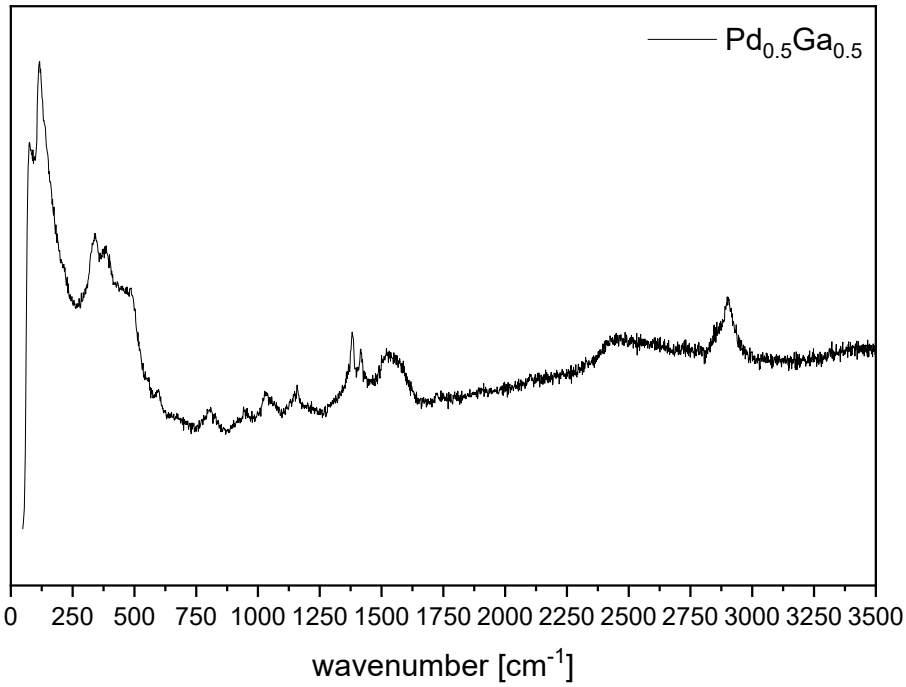

Figure S15. Raman measurement of the $Pd_{0.5}Ga_{0.5}$ colloids after precipitation at 25°C.

PXRD measurements

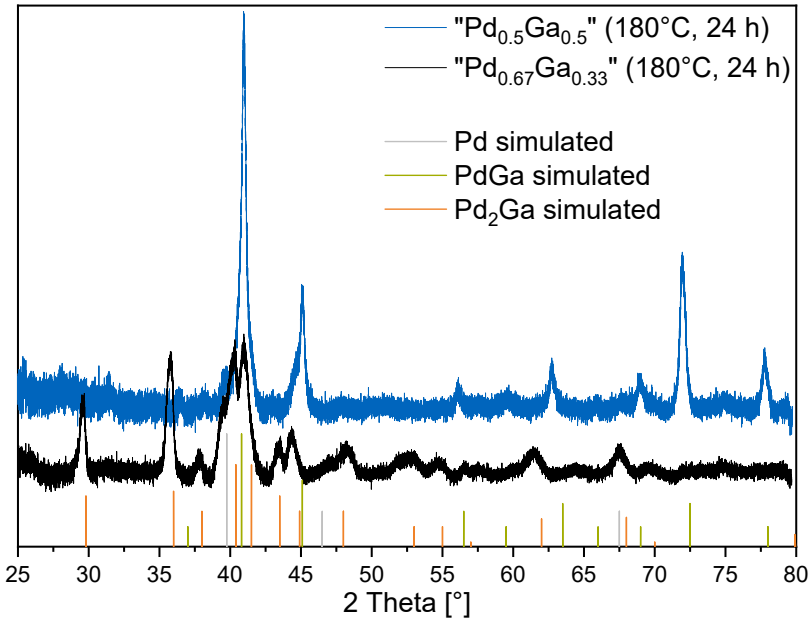

Figure S16. PXRD measurements of the precipitated $Pd_{1-x}Ga_x$ colloids. For crystallinity, samples were annealed in vacuum at 180°C for 24 h prior to measurements. Without annealing, no reflexes could be detected. For Pd/Ga = 1:2, a X-ray diffractometric phase determination was not successful due to the poor crystallinity of the sample.

Elemental analysis

Table S2. ICP-MS measurements of the colloids.

Sample	Pd : Ga (calculated)	Pd : Ga (measured)
$Pd_{0.67}Ga_{0.33}$	2 : 1	2.52 ± 0.01 : 1
$Pd_{0.5}Ga_{0.5}$	1 : 1	1.13 ± 0.00 : 1
$Pd_{0.33}Ga_{0.67}$	0.5 : 1	0.60 ± 0.00 : 1

For preparation, all volatile compounds were removed in vacuo. ICP-MS measurements for all samples show a slightly too low value of Ga. This can be attributed to the synthesis set-up, as the liquid precursor GaCp* is added to the reaction mixture with a syringe, always leaving a small residue in there.

Table S3. Atomic-absorption spectroscopy (AAS) analysis of the precipitated $Pd_{1-x}Ga_x$ colloids.

Sample	Pd : Ga (calculated)	Pd : Ga (measured)
$Pd_{0.67}Ga_{0.33}$	2 : 1	3 : 1
$Pd_{0.5}Ga_{0.5}$	1 : 1	1.4 : 1
$Pd_{0.33}Ga_{0.67}$	0.5 : 1	1 : 1

For all samples, insoluble white residues were observed, which can probably be identified as Ga oxide species. Hence, the Ga content is in all samples underestimated.

2. Catalytic performance of $Pd_{1-x}Ga_x$ (x = 0.67, 0.5, 0.33) colloids in the semi-hydrogenation of alkynes

Error calculation

c = conversion, y = yield, s = selectivity (all denoted in %)

$$s = \frac{y}{c}$$

$$\Delta s = \sqrt{\left(\frac{\partial s}{\partial c} \cdot \Delta c\right)^2 + \left(\frac{\partial s}{\partial y} \cdot \Delta y\right)^2}$$

Table S4. Example for an error calculation for the selectivities using 5 mol% $Pd_{0.5}Ga_{0.5}$ colloids (Pd/Ga = 1:1) at 0 °C and 1.0 bar H_2 assuming an instrumental NMR inaccuracy of 1 % due to overlapping of alkyne/alkene/alkane signals.

Time [h]	c	Δc	y	Δy	s	$\left(\frac{\partial s}{\partial c} \cdot \Delta c\right)$	$\left(\frac{\partial s}{\partial y} \cdot \Delta y\right)$	Δs (percentaged)	Δs (absolute)
1	24	0,24	24	0,24	100	0,01	0,01	0,014142136	1,41
2	39	0,39	34	0,34	86	0,008717949	0,008717949	0,012329041	1,06
3	45	0,45	40	0,44	84	0,009777778	0,008888889	0,013214283	1,11
4	50	0,5	43	0,43	85	0,0086	0,0086	0,012162237	1,03
5	59	0,59	48	0,48	81	0,008135593	0,008135593	0,011505466	0,94
6	65	0,65	53	0,53	81	0,008153846	0,008153846	0,01153128	0,93

The highest error of the selectivity of Δs = ±1.41% is too low to have an influence on the interpretation of the following catalytic test and therefore were not considered.

Catalyst stability during catalysis: NMR study

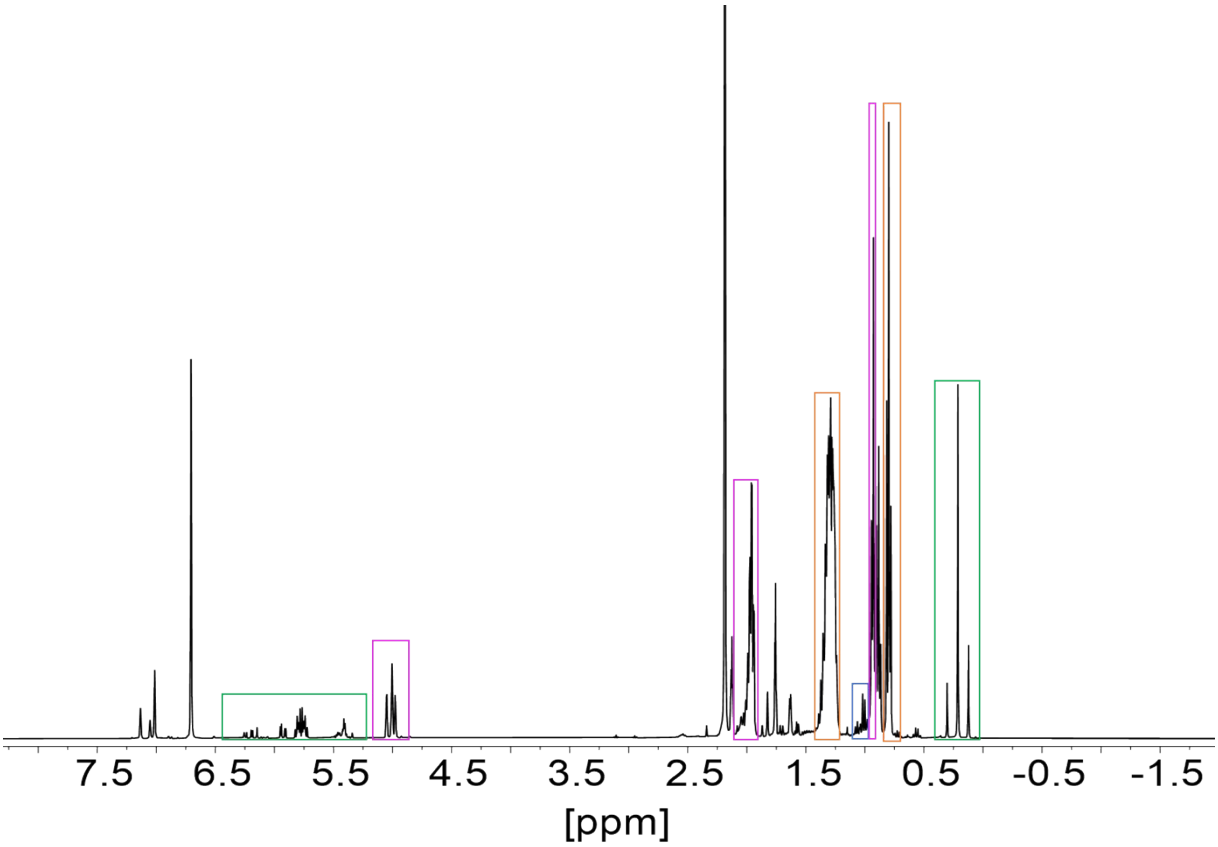

Figure S17. ^{1}H NMR study of $Pd_{0.5}Ga_{0.5}$ colloids during semi-hydrogenation catalysis of 3-hexyne (5 mol% catalyst, 0°C, 1 bar H_2, 8 h) after 74 % conversion showing small amounts of dvds hydrogenation (signal at 0.11 ppm, 6 H, C*H*$_3$). Color code: Dvds in green, 3-hexyne in blue, 3-hexene in purple, *n*-hexane in orange. ^{1}H NMR (400 MHz, toluene-*d*$_8$): 7.11-6.98 (m, residual signal of toluene-*d*$_8$), 6.68 (s, 3H, internal standard mesitylene, CH), 5.92 (m, 6H, dvds, C*H*, C*H*$_2$), 4.97 (t, 2H, 3-hexene, C*H*), 2.15 (s, 9H, internal standard mesitylene, C*H*$_3$), 1.92 (m, 4H, 3-hexene, C*H*$_2$), 1.76 (m, Cp*H, 12H, C*H*$_3$), 1.25 (m, 8H, *n*-hexane, C*H*$_2$), 1.01 (t, 6H, 3-hexyne, C*H*$_3$), 0.91 (t, 6H, 3-hexene, C*H*$_3$), 0.79 (t, 6H, *n*-hexane, C*H*$_3$), 0.53 (q, ^{3}J = 8.0 Hz, Cp*H, 1H, C*H*), 0.18 (s, dvds, 12H, C*H*$_3$).

Parameter optimization

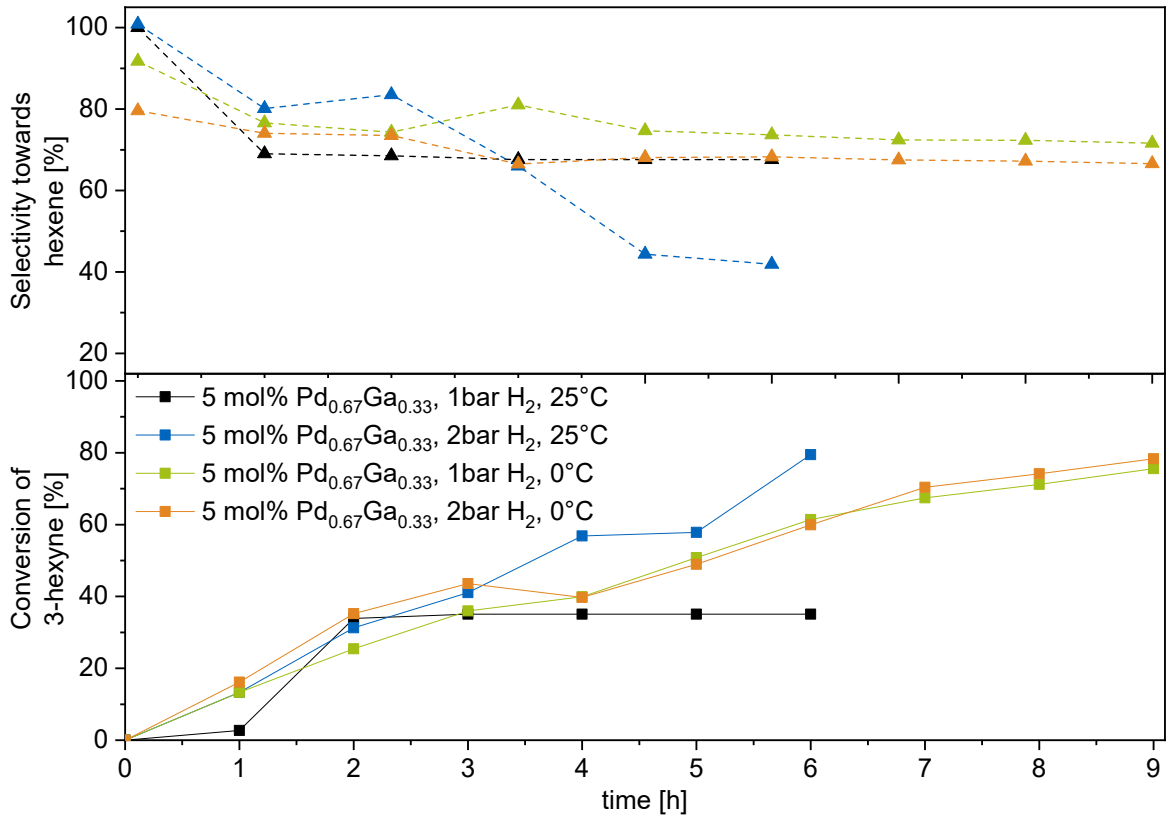

Figure S18. Parameter optimization regarding the semi-hydrogenation catalysis using $Pd_{0.67}Ga_{0.33}$ colloids. At 25 °C (Entry 1 and 2), partial particle precipitation and dvds hydrogenation is observed. Entry 1: Complete H_2 consumption after 2 h.

Variation of the catalyst amount

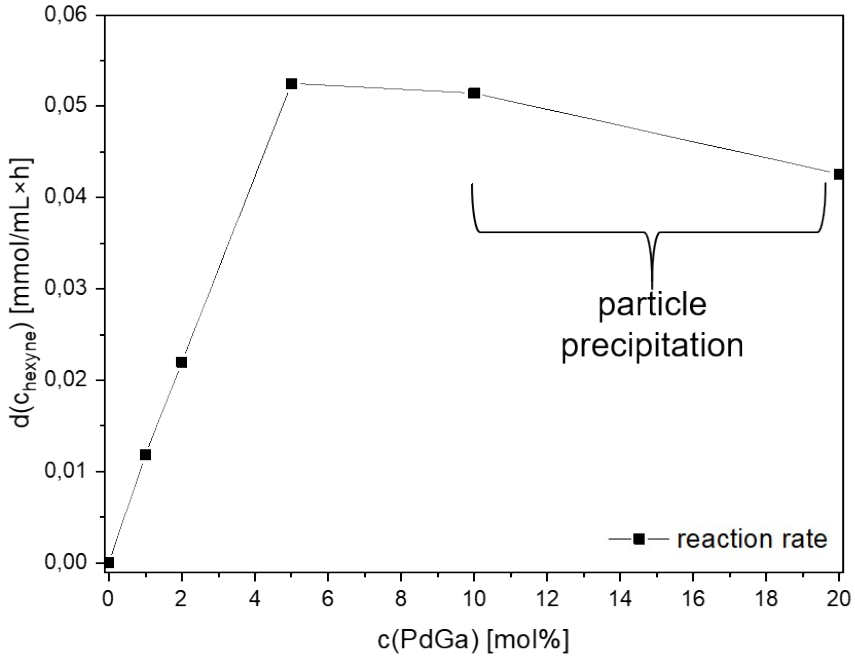

Figure S19. Variation of the catalyst amount using $Pd_{0.5}Ga_{0.5}$ colloids highlighting 5 mol% catalyst as optimum.

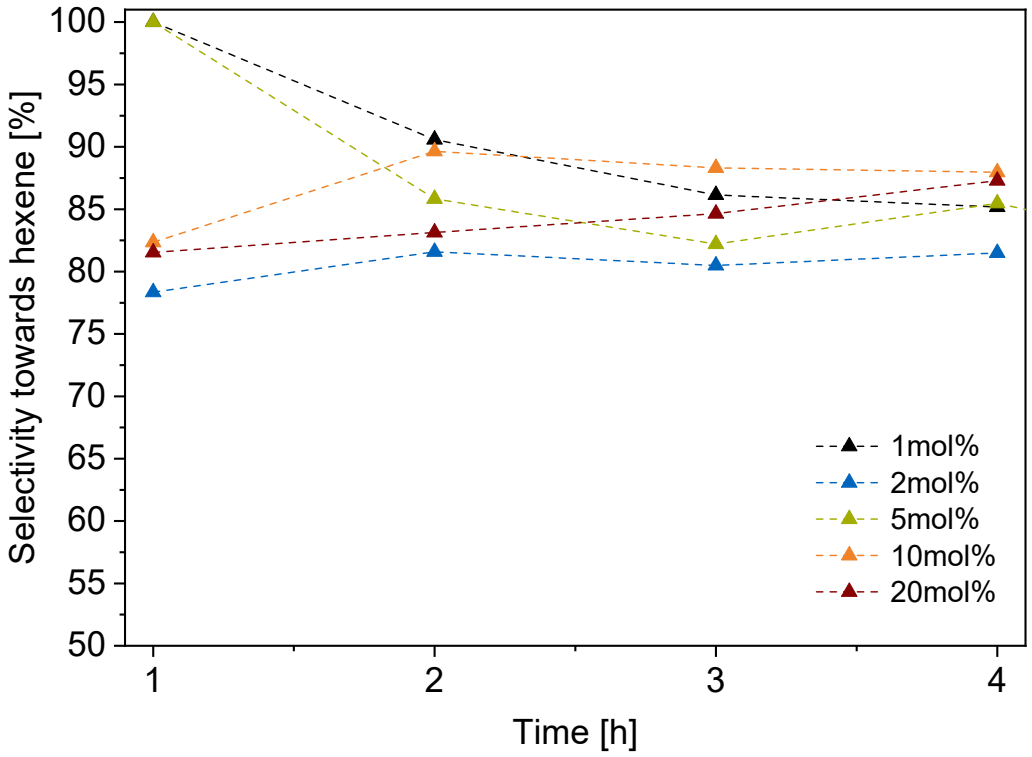

Figure S20. Influence of the loading of the colloidal $Pd_{0.5}Ga_{0.5}$ catalyst on the selectivity by variation of the catalyst amount using $Pd_{0.5}Ga_{0.5}$ colloids.

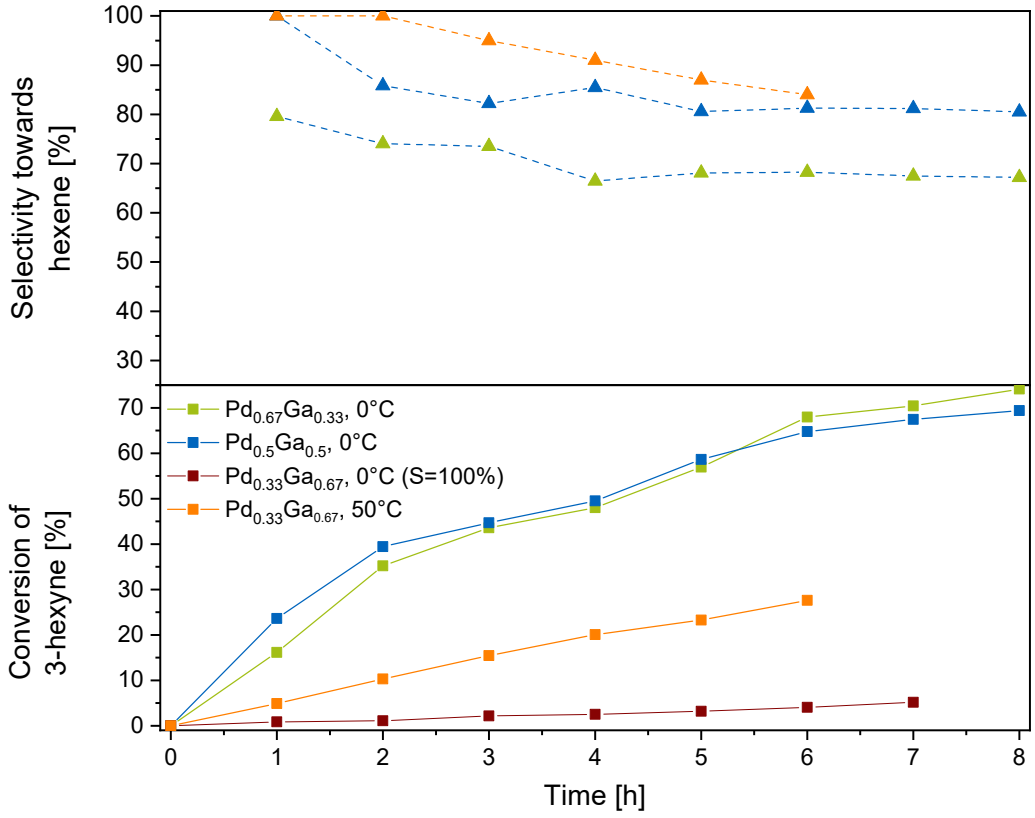

Figure S21. Testing of the catalytic performance of $Pd_{1-x}Ga_x$ NPs in the semi-hydrogenation of 3-hexyne with different Pd/Ga ratios using 5 mol% catalyst.

Calculation of rate constants

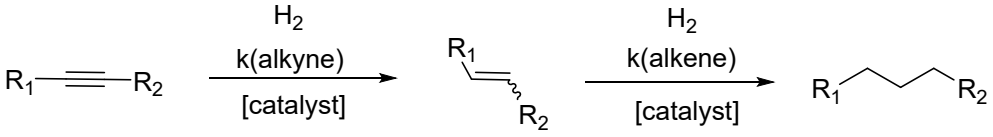

$$r = \frac{dc(alkyne)}{dt} = k(alkyne) \cdot c(alkyne)$$

Table S5. Calculated ratio of the rate constants k(alkyne) and k(alkene). Catalytic tests were performed using 5 mol% $Pd_{0.67}Ga_{0.33}$ as catalyst with 3-hexyne as substrate at 0°C and 2.0 bar H_2.

Reaction time [h]	$\frac{k(alkyne)}{k(alkene)}$
1 → 2	2.873
2 → 3	2.932
3 → 4	2.918
4 → 5	2.635
5 → 6	2.706
6 → 7	2.062

Table S6. Calculated ratio of the rate constants k(alkyne) and k(alkene). Catalytic tests were performed using 5 mol% $Pd_{0.5}Ga_{0.5}$ as catalyst with 3-hexyne as substrate at 0°C and 2.0 bar H_2.

Reaction time [h]	$\frac{k(alkyne)}{k(alkene)}$
1 → 2	3.253
2 → 3	3.193
3 → 4	3.238
4 → 5	3.162
5 → 6	2.678
6 → 7	2.348

Substrate variation

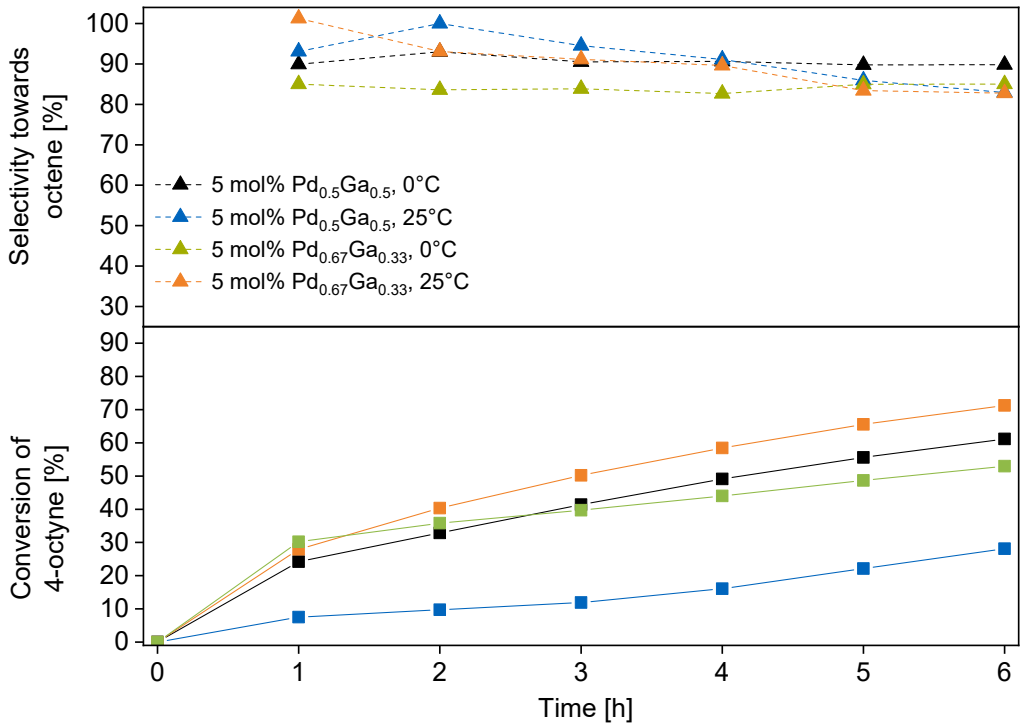

Figure S22. Semi-hydrogenation of 4-octyne as substrate using 5mol% $Pd_{1-x}Ga_x$ colloids and 2.0 bar H_2 at various temperatures.

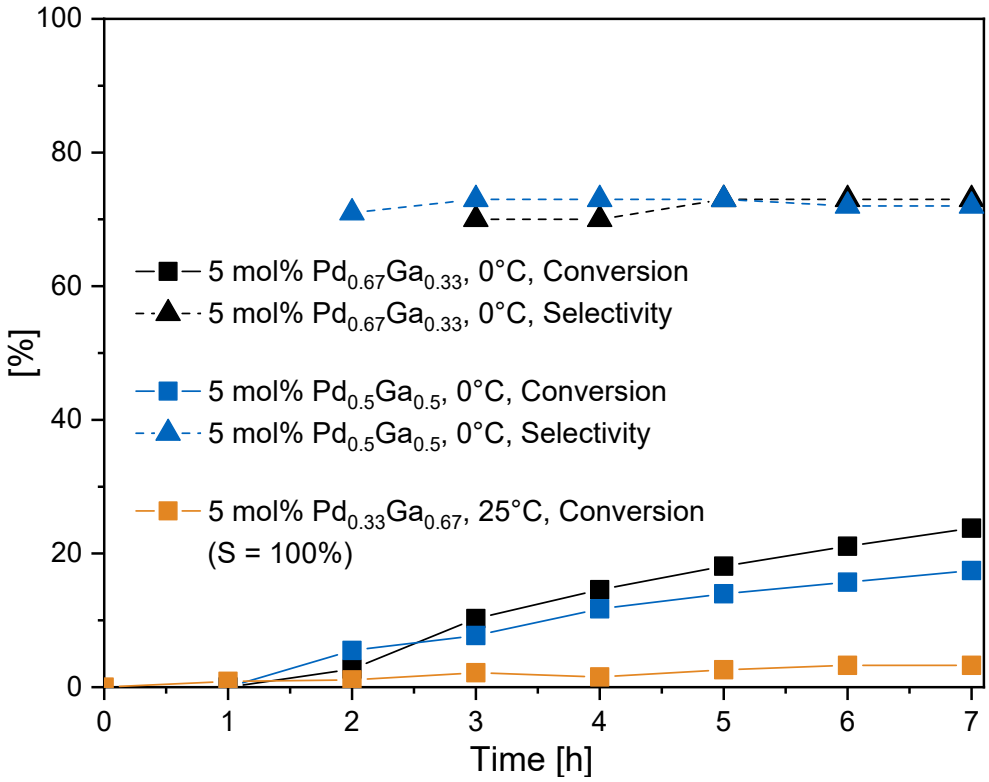

Figure S23. Catalytic tests on the semi-hydrogenation of 1-hexyne as substrate using $Pd_{1-x}Ga_x$ colloids and 2.0 bar H_2 showing a strong increase of the catalyst activity.

Substrate oligomerization using terminal alkynes

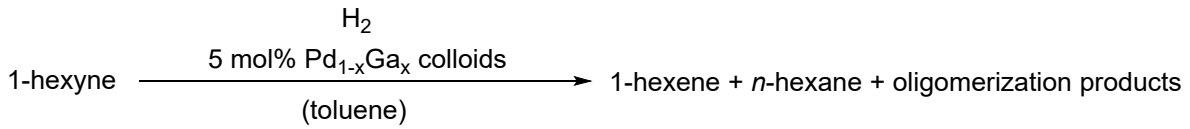

Scheme S1. Reaction scheme for the hydrogenation of the terminal alkyne 1-hexyne including undesired oligomerization processes during catalysis.

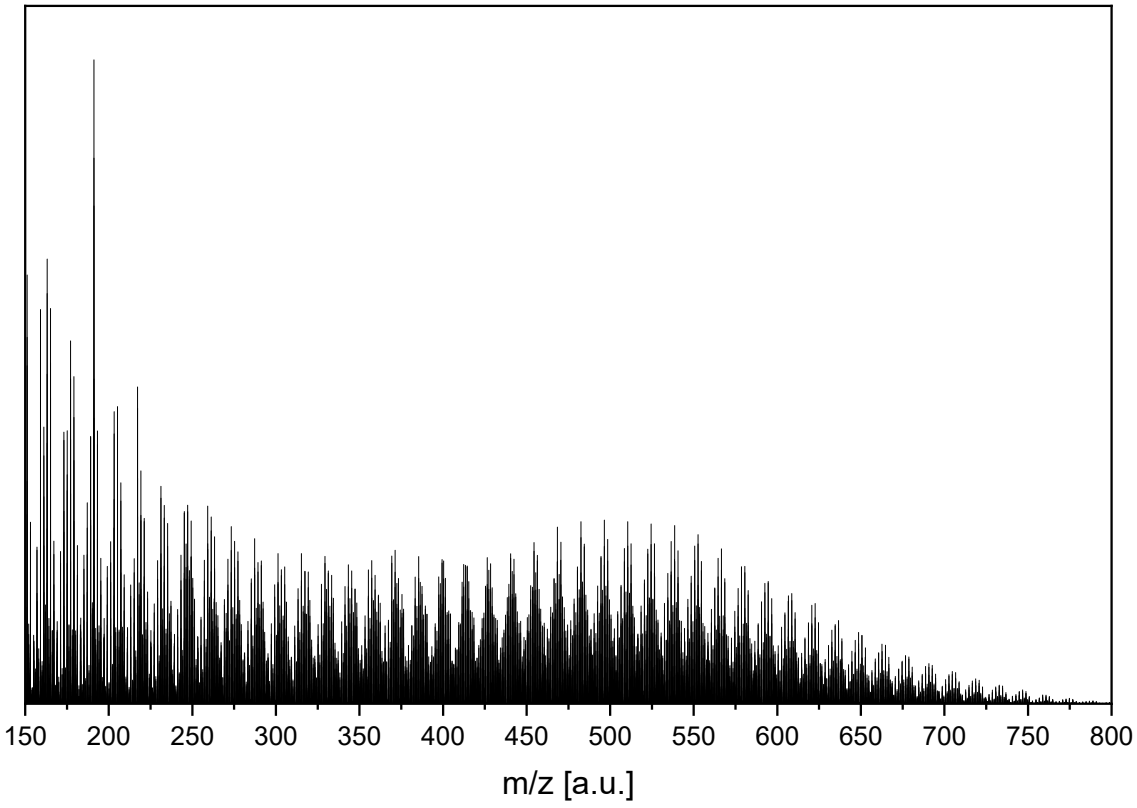

Figure S24. LIFDI-MS measurements of the reaction mixture after catalysis using 5mol% $Pd_{0.5}Ga_{0.5}$ colloids, 2.0 bar H_2 at 0°C and 1-hexyne as substrate showing strong oligomerization.

Calculation of TOF values and comparison with literature-known systems

Calculation of TOF values: TOF [h^{-1}] = $\frac{conversion\ (after\ 1\ h) \times n_0(alkyne)}{n(cat) \times 1\ h}$

whereas n(cat) = $\frac{n(all\ Pd) \times 0{,}764\ (Pd\ surface\ atoms)}{Pd/Ga\ ratio}$

The amount of Pd surface atoms was calculated based on the model of magic cluster numbers, with a Pd NP diameter of 1.5 nm. Here, in a monometallic Pd NP 76.4% of all Pd atoms are located on the surface. This value was then approximated to the corresponding Pd/Ga ratio; etc. for Pd/Ga = 1:1, the amount of active Pd atoms on the surface was divided by the factor 2. It must be mentioned that this calculation is only an approximation, as the core-shell structure of the particles was not considered, why the amount of active Pd surface atoms is rather overestimated and therefore the TOF value underestimated.

Table S7. Calculation of TOF values using 5mol% $Pd_{1-x}Ga_x$, 1 bar H_2 at 0 °C.

Entry	Conversion	n_0(alkyne) [mol]	n(cat) [mol]	TOF [h^{-1}]
$Pd_{0.67}Ga_{0.33}$, 3-hexyne	0,26	0,0000277	$5{,}72 \times 10^{-8}$	126
$Pd_{0.5}Ga_{0.5}$, 3-hexyne	0,24	0,0000277	$4{,}33 \times 10^{-8}$	153
$Pd_{0.33}Ga_{0.67}$, 3-hexyne	0,05	0,0000277	$3{,}49 \times 10^{-8}$	40
$Pd_{0.67}Ga_{0.33}$, 4-octyne	0,30	0,0000277	$5{,}72 \times 10^{-8}$	146
$Pd_{0.5}Ga_{0.5}$, 4-octyne	0,24	0,0000277	$4{,}33 \times 10^{-8}$	155
$Pd_{0.67}Ga_{0.33}$, 1-hexyne	0,05	0,0000277	$5{,}72 \times 10^{-8}$	24
$Pd_{0.5}Ga_{0.5}$, 1-hexyne	0,03	0,0000277	$4{,}33 \times 10^{-8}$	19
$Pd_{0.33}Ga_{0.67}$, 1-hexyne	0,01	0,0000277	$3{,}49 \times 10^{-8}$	10

Table S8. Comparison of literature-known TOF values for hydrogenation reactions using small monometallic Pd NPs and heterogeneous Pd/Ga systems.

Ref.	Metal/capping agent	NP size [nm]	Reaction type	Substrate	Reaction conditions	TOF [h^{-1}]	Conv.	Sel. [%]
[S1]	Pd@PVP (1:100)	1.7±0.3	Semi-hydrogenation	1-hexyne	25°C, $p(H_2)$ = 1bar	1320	100 % after 5 h	93
				2-hexyne		23400	100 % after 40 min	90
				3-hexyne		12600	100 % after 30 min	95
[S2]	Pd@PVP (1: 20)	2.1±0.1	Semi-hydrogenation	dehydroisophytol	40°C, $p(H_2)$ = 4bar	42840	100 %	96
				methylbutenol		48780	100 %	98
[S2]	Pd@PVP (1:10)	3.6±0.4	Semi-hydrogenation	dehydroisophytol	40°C, $p(H_2)$ = 4bar	69120	100 %	89
				methylbutenol		78960	100 %	98
[S3]	Pd@(BCN)MI(NTf_2)	7.3±2.2	Semi-hydrogenation	diphenylacetylene	25°C, $p(H_2)$ = 1bar	13	87 % after 6.5 h	98
				phenylacetylene		35	97 % after 2.8 h	95
				3-hexyne		231	100 % after 1.3 h	92
[S5]	Pd@SC_8	2.3	Selective hydrogenation of dienes	2,3-dimethylbuta-1,3-diene	25°C, $p(H_2)$ = 1bar	375	100 % after 24 h	100
[S5]	Pt@SC_{12}	1.5	Full-hydrogenation	Methyl propiolate	25°C, $p(H_2)$ = 1bar	30	100 % after 24 h	“high”
[S6]	Pd_2Ga	-	Semi-hydrogenation	Acetylene	200°C, flow reactor (5% H_2)	58	93 % after 20 h	76
[S6]	PdGa	-	Semi-hydrogenation	Acetylene	200°C, flow reactor (5% H_2)	1	86 % after 20 h	75
[S6]	Pd_3Ga_7	-	Semi-hydrogenation	Acetylene	200°C, flow reactor (5% H_2)	1	99 % after 20 h	71
[S6]	Pd@Al_2O_3	-	Semi-hydrogenation	Acetylene	200°C, flow reactor (5% H_2)	2452	43 % after 20 h	17
[S6]	Pd_2Ga@Al_2O_3	2-6	Semi-hydrogenation	Acetylene	200°C, flow reactor (5% H_2)	6615	88 % after 20 h	67

3. Analysis of the $Pd_{1-x}Ga_x$ (x = 0.67, 0.5, 0.33) colloids after catalysis runs

HR-TEM measurements

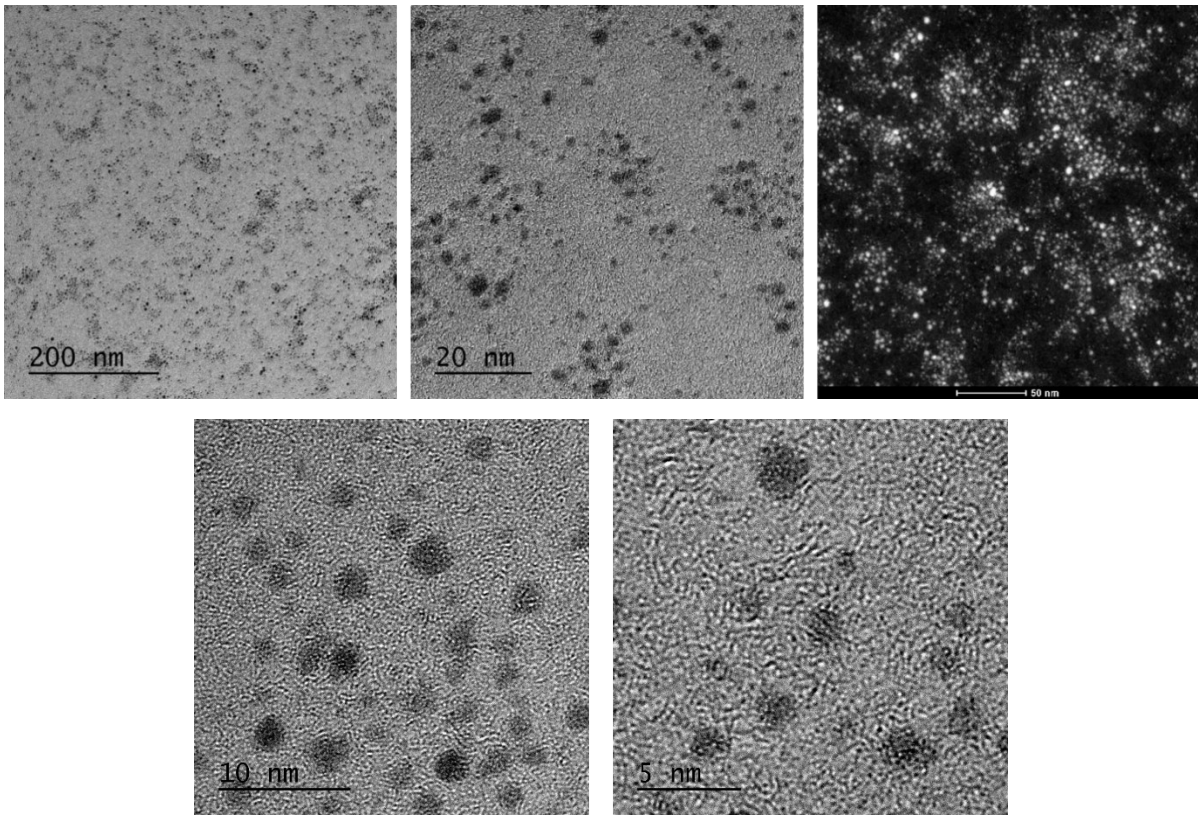

Figure S26. HR-TEM image and HAADF of $Pd_{0.5}Ga_{0.5}$ colloids after semi-hydrogenation catalysis of 3-hexyne at 0°C and 2.0 bar H_2 after 5 h.

DLS measurements

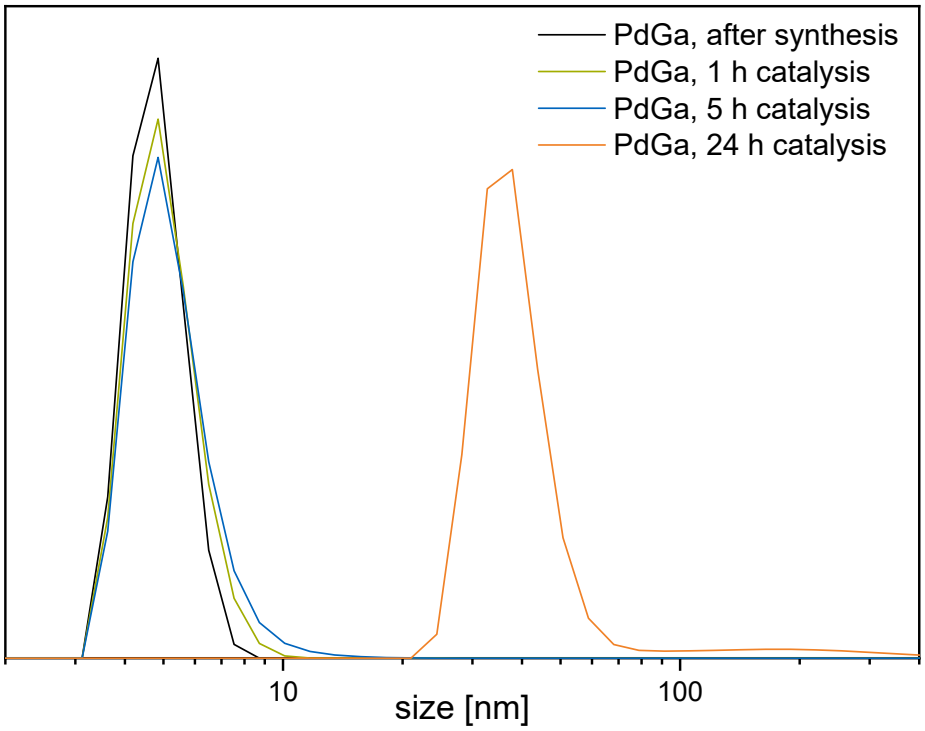

Figure S27. DLS monitoring of $Pd_{0.5}Ga_{0.5}$ colloids during the semi-hydrogenation of 3-hexyne at 0°C and 2.0 bar H_2.

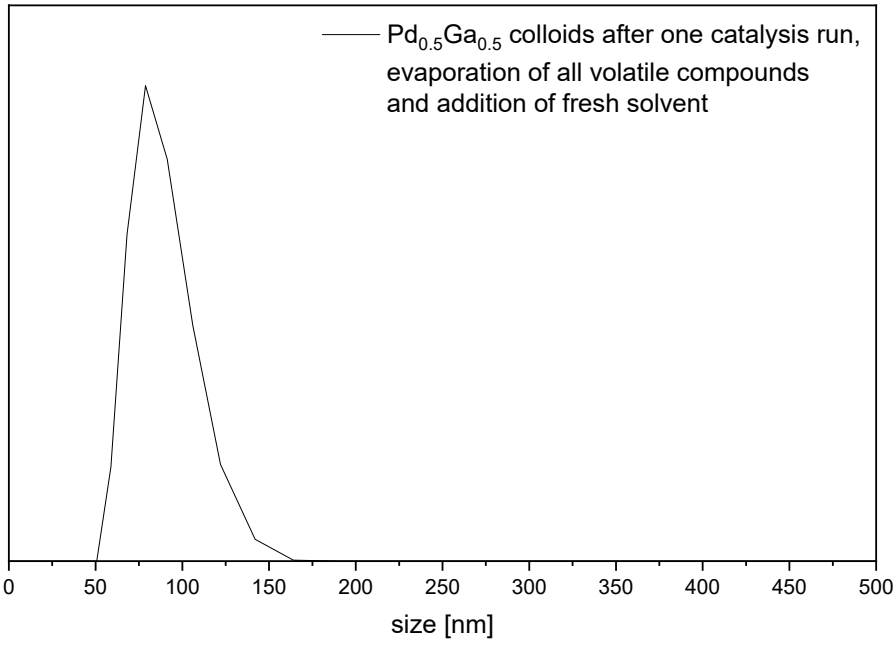

Figure S28. DLS measurements of $Pd_{0.5}Ga_{0.5}$ colloids after one catalysis run, evaporation of all volatile compounds and addition of fresh solvent and substrate showing agglomeration.

A loss of catalytic activity for the second run is observed for longer reaction times, which can be explained with a particle agglomeration with NP sizes around 80 nm according to DLS measurements. This rather high degree of agglomeration can be attributed to the sample preparation, as after the first run, all volatile compounds were removed in vacuo leading to an increased particle destabilization and agglomeration.

IR measurements

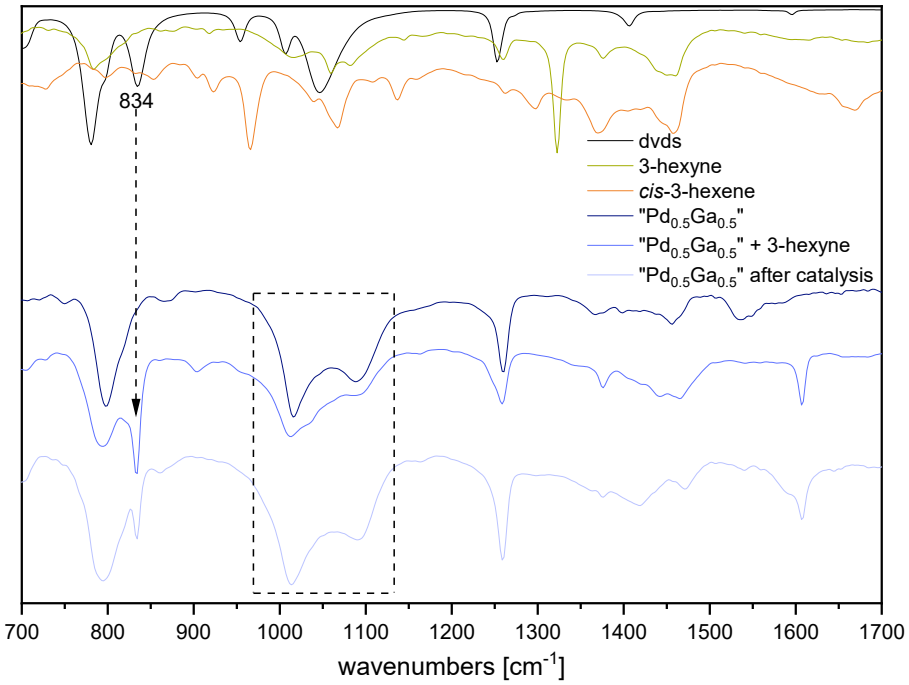

Figure S29. ATR FT-IR measurement of the $Pd_{0.5}Ga_{0.5}$ colloids upon addition of 3-hexyne and after catalysis runs (bottom traces, blue) and pure dvds and Cp*H as reference (upper traces, black, green and orange).

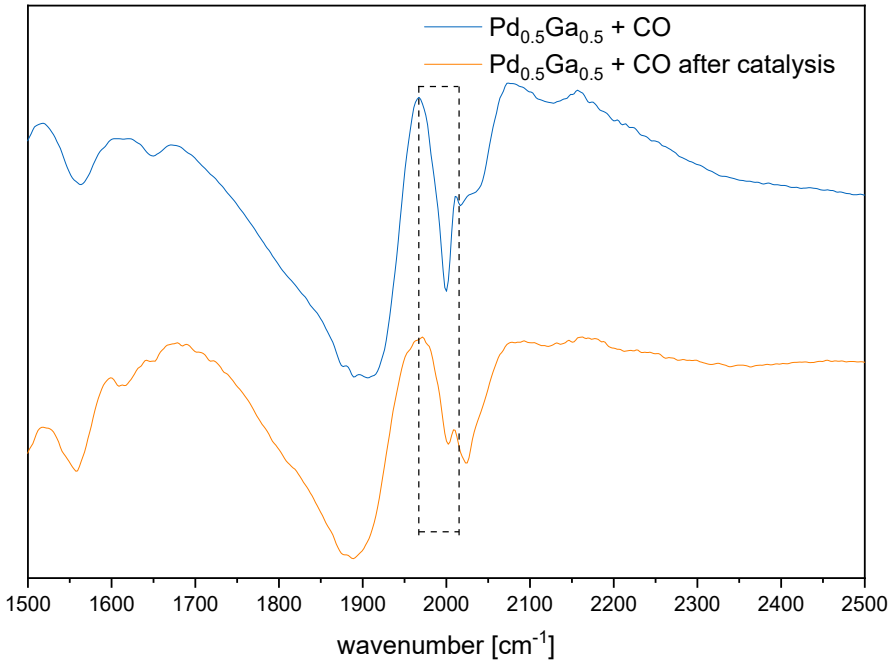

Figure S30. ATR FT-IR measurement of the $Pd_{0.5}Ga_{0.5}$ colloids upon addition of CO before (blue trace) and after (orange trace) the catalytic semi-hydrogenation of 3-hexyne showing a decrease of the signal at 2000 cm^{-1} typical for linearly bonded CO.

4. References

[S1] C. Evangelisti, N. Panziera, A. D'Alessio, L. Bertinetti, M. Botavina, G. Vitulli, *J. Catal.* **2010**, *272*, 246–252.

[S2] A. Yarulin, I. Yuranov, F. Cardenas-Lizana, P. Abdulkin, L. Kiwi-Minsker, *J. Phys. Chem. C* **2013**, *117*, 13424–13434.

[S3] R. Venkatesan, M. H. G. Prechtl, J. D. Scholten, R. P. Pezzi, G. Machadoc, J. Dupont, *J. Mater. Chem.* **2011**, *21*, 3030–3036.

[S4] T. Chen, Y. S. Shon, *Catal. Sci. Technol.* **2017**, *7,* 4823–4829.

[S5] K. A. San, V. Chen, Y.-S. Shon, *ACS Appl. Mater. Interfaces* **2017**, *911*, 9823–9832.

[S6] a) M. Armbrüster, M. Behrens, D. Teschner, Y. Grin, R. Schlögl, *J. Am. Chem. Soc.* **2010**, *132*, 42, 14745–14747; b) M. Armbrüster**,** K. Kovnir, M. Behrens, D. Teschner, Y. Grin, R. Schlögl, *JACS* **2010**, *132*, 14745-14747.